Published for SISSA by Springer

Received: November 30, 2024
Revised: February 28, 2025
Accepted: March 15, 2025
Published: April 11, 2025

Symmetry-resolved relative entropy of random states

Mostafa Ghasemi

Research Center for High Energy Physics, Department of Physics, Sharif University of Technology, P.O.Box 11155-9161, Tehran, Iran
School of Particles and Accelerators, Institute for Research in Fundamental Sciences (IPM), P.O. Box 19395-5531, Tehran, Iran

E-mail: ghasemi.mg@ipm.ir

Abstract: We use large-N diagrammatic techniques to calculate the relative entropy of symmetric random states drawn from the Wishart ensemble. These methods are specifically designed for symmetric sectors, allowing us to determine the relative entropy for random states exhibiting U(1) symmetry. This calculation serves as a measure of distinguishability within the symmetry sectors of random states. Our findings reveal that the symmetry-resolved relative entropy of random pure states displays universal statistical behavior. A remarkable finding is that relative entropies violate entanglement equipartition in the symmetry resolution for Haar-random states. Finally, we derive the symmetry-resolved Page curve. These results deepen our understanding of the properties of these random states.

Keywords: Global Symmetries, Matrix Models, Random Systems

ArXiv ePrint: 2411.01491

https://doi.org/10.1007/JHEP04(2025)090

JHEP04(2025)090

Contents

JHEP04(2025)090

1 Introduction

Random Matrix Theory (RMT) is a mathematical framework that studies the properties of matrices whose entries are random variables. It is a ubiquitous topic in mathematics and quantum physics [1–3]. RMT has significant implications across various fields, ranging from statistics, number theory, and combinatorics to characterizing the dynamics of chaotic quantum many-body systems and thermalization [4], quantum information [5], the foundations of statistical mechanics [6, 7], and providing toy models for the black hole information problem [8, 9].

A random quantum state is a state that is sampled according to some random distribution, typically the uniform (Haar) distribution on the space of pure states or the space of density matrices for mixed states. One of the main structures studied in the realm of random states is the quantum entanglement structure. The entanglement structure of random states was initially explored in the work of Page [10], where the average von Neumann entanglement entropy of random pure states distributed according to the Haar measure was considered. For the bipartite system $A \cup \bar{A}$, and a large Hilbert space $\mathcal{H} = \mathcal{H}_A \otimes \mathcal{H}_{\bar{A}}$, Page's formula gives

$$\mathcal{S} \approx \min\left(\log d_A, \log d_{\bar{A}}\right) + \cdots . \tag{1.1}$$

Here, d_A and $d_{\bar{A}}$ represent the dimensions of $\mathcal{H}_A$ and $\mathcal{H}_{\bar{A}}$, respectively. The average entanglement entropy of a subsystem, up to subleading corrections, is maximal. This implies that the bipartite entanglement entropy of typical states is nearly maximal. When plotted against the subsystem's size, the average entanglement entropy forms a Page curve. The Page curve describes how the entanglement entropy of Hawking radiation evolves over time as a black hole evaporates. Initially, it increases but eventually decreases as the black hole loses information, providing insights into how information might be recovered from black holes. Page's formula provides a qualitative description for the behavior of typical Hamiltonians or states generated by sufficiently chaotic dynamics. It is believed that these systems can be well described by random states. For a detailed review, refer to [4, 11].

Another quantum information- theoretic quantity that can be useful in this context is the relative entropy. Relative entropy is a measure of distinguishability for quantum states and is essential in quantum information theory [12] and quantum statistical mechanics [13]. Relative entropy has favorable properties, like monotonicity and positivity. These properties, make the relative entropy a valuable tool in various areas of physics, including quantum field theory [14–17], conformal field theory [18–21], boundary conformal field theory [22] holography [23–26], quantum gravity [27–31], and random states [32, 33].

The relative entropy between two density matrices ρ and σ is defined as

$$D(\rho||\sigma) := \mathrm{Tr}\left[\rho\left(\log\rho - \log\sigma\right)\right]. \tag{1.2}$$

Here, $D(\rho||\sigma) = 0$ if and only if $\rho = \sigma$. Importantly, the relative entropy is monotonic under quantum operations [35]

$$D(\mathcal{N}(\rho)||\mathcal{N}(\sigma)) \leq D(\rho||\sigma), \tag{1.3}$$

where $\mathcal{N}$ represents any completely-positive trace-preserving map. A significant quantum operation is the partial trace, and monotonicity in this context implies that density matrices become less distinguishable as more information about them is discarded. In this context, the author [32] calculates the relative entropy for Haar random states using a large-N diagrammatic technique,

$$D(\rho_A||\sigma_A) = 1 + \frac{d_A}{2d_{\bar{A}}} + \left(\frac{d_{\bar{A}}}{d_A} - 1\right)\log\left(1 - \frac{d_A}{d_{\bar{A}}}\right). \tag{1.4}$$

The relative entropy increases monotonically with $d_A/d_{\bar{A}}$ and reaches a value of 3/2 when $d_A = d_{\bar{A}}$. This behavior, as expected, demonstrates the monotonicity of relative entropy under the partial trace.

Quantum chaos and thermalization are intriguing concepts in quantum physics that relate to distinguishability, randomness in states, and the behavior of quantum systems as they evolve over time. Random states are typical states in high-dimensional Hilbert spaces and play a crucial role in understanding the behavior of thermalized quantum systems. As quantum systems evolve chaotically, their states become increasingly random, resembling thermal states. Relative entropy is a useful tool for tracking the loss of information in quantum chaotic systems. As a chaotic system evolves, information about its initial state becomes scrambled and lost, making the state more random and more similar to a thermal state. Random states, being effectively indistinguishable from thermal states, have low relative entropy with respect to the thermal state. In the presence of symmetry, it is interesting to explore the distinguishability within each symmetry sector. In the next section, we will address the interplay between symmetry and entanglement.

1.1 Symmetry-resolved relative entropy

Entanglement and symmetry are two pillars of modern physics. One interesting problem in this context involves understanding the relationship between entanglement and symmetry. The presence of symmetry can impact the distribution of entanglement. It's important to explore how entanglement is distributed within the symmetry sectors of a theory. One of the main tools used to study this is the symmetry-resolved entanglement entropy [36],

JHEP04(2025)090

which determines the contribution of each symmetry sector associated with a given global symmetry to the total entanglement entropy.

More generally, in the presence of a global symmetry, the density matrix ρ of the total system commutes with a conserved charge $\hat{Q}$, $[\rho, \hat{Q}] = 0$. By tracing over the degrees of freedom of the subsystem $\bar{A}$, we find that $[\rho_A, \hat{Q}_A] = 0$, where $\hat{Q}_A$ is the total charge in the A subsystem. This means that the reduced density matrix ρ_A can be decomposed into block diagonal form associated with each charge sector,

$$\rho_A = \bigoplus_Q P(Q_A)\rho_A(Q_A), \tag{1.5}$$

and the charged partition function becomes

$$\mathcal{Z}_n(Q_A) = \mathrm{Tr}\rho_A^n \Pi_A^{(Q)} = \int_{-\pi}^{\pi} \frac{\mathrm{d}\alpha}{2\pi} \mathcal{Z}_n(\alpha) e^{-i\alpha Q_A}. \tag{1.6}$$

where $\mathcal{Z}_n(\alpha)$ is the so-called charged moment. $\Pi_A^{(Q)}$ denotes the projection into the subspace of states of region A with charge $\hat{Q}_A$. Symmetry-resolved Rényi entropies are defined as,

$$S_n(Q_A) = \frac{1}{1-n} \log\left[\frac{\mathcal{Z}_n(Q_A)}{\mathcal{Z}_1^n(Q_A)}\right], \tag{1.7}$$

and symmetry-resolved entanglement entropy is obtained as,

$$S(Q_A) = \lim_{n \to 1} S_n(Q_A). \tag{1.8}$$

Probability is then recovered as $P(Q_A) = \mathcal{Z}_1(Q_A)$. Regarding the decomposition of the reduced density matrix (1.5), the total entanglement entropy can be divided into two terms,

$$\begin{aligned} S_E &= \sum_{Q_A} P(Q_A) S(Q_A) - \sum_{Q_A} P(Q_A) \log(P(Q_A)) \\ &= S^c + S^n. \end{aligned} \tag{1.9}$$

S^c represents the configurational entropy [37], which is defined as the weighted sum of the entropies in each sector. On the other hand, S^n, known as the number entropy [37–40], quantifies the entropy caused by the fluctuations of charge within subsystem A.

Over the past few years, this subject has been the focus of intense research activity, including studies on topics such as 1+1-dimensional conformal field theories [36, 41–48]. Additionally see [49–59] for further references. One main feature emerging from the literature is that, due to conformal invariance, the entanglement entropy is equally distributed among different sectors. Strictly speaking, at the leading order, the symmetry-resolved entanglement entropy is independent of the charge sector.

Similar to symmetry-resolved entanglement entropy, the concept of symmetry-resolved relative entropy (SRRE) can be defined [60, 61]. Symmetry-resolved relative entropy provides measures of the distinguishability of two states within the same symmetry sector. For two reduced density matrices, denoted as ρ and σ, the symmetry-resolved relative entropy corresponds to each sector Q defined as

$$D(\rho(Q)||\sigma(Q)) := \mathrm{Tr}\left[\rho(Q)\left(\log\rho(Q) - \log\sigma(Q)\right)\right]. \tag{1.10}$$

JHEP04(2025)090

The symmetry-resolved relative entropies satisfy the sum rule,

$$D(\rho||\sigma) = \sum_Q P^\rho(Q) D(\rho(Q)||\sigma(Q)) + \sum_Q P^\rho(Q) \log \frac{P^\rho(Q)}{P^\sigma(Q)} \tag{1.11}$$

where $P^\rho(Q) \equiv \mathrm{tr}\left(\rho \Pi^Q\right)$ and $P^\sigma(Q) \equiv \mathrm{tr}\left(\sigma \Pi^Q\right)$. From a replica perspective, the symmetry-resolved relative entropy can be obtained as the replica limit $n \to 1$ of the n-th Rényi entropy of the sector Q,

$$D(\rho(Q)||\sigma(Q)) = -\partial_n \log \left(\frac{\mathrm{Tr}\left(\rho(Q)\sigma^{n-1}(Q)\right)}{\mathrm{tr}\rho^n(Q)} \right) \Big|_{n\to 1}. \tag{1.12}$$

The interesting question that motivated this work is: what is the thermalization process in individual system charge sectors? Quantum thermalization in isolated many-body systems with global symmetry, and the charged black hole information problem, motivate us to study the relative entropy of symmetric random quantum states. A more fundamental quantity in this context is the symmetry-resolved relative entropy. It not only encodes information about the interplay between symmetry and entanglement, but also provides the statistical distance between two states in a given symmetry sector. In this work, we investigate the symmetry-resolved relative entropy in the Haar-random states with a U(1) symmetry. Since X is a Gaussian random variable, all of its moments can be decomposed in terms of its second moment. Using the large-N diagrammatic techniques, we derive explicit analytic formulas for the corresponding symmetry-resolved Page curves and symmetry-resolved relative entropy. This paper is organized as follows: in section 2, we introduce the U(1) symmetric random states and evaluate the symmetry-resolved Page curve. In section 3, we evaluate the symmetry-resolved relative entropy for the U(1) symmetric random states. A summary of the results and further directions for research are included in section 4.

2 Symmetric random pure states

In this section, we will study an ensemble of Haar random pure states with a U(1) charge and generator $\hat{Q}$ based on the diagrammatic approach [32–34]. Given a global symmetry, the Hilbert space can be decomposed as:

$$\mathcal{H} = \bigoplus_{Q=0} \mathcal{H}(Q), \tag{2.1}$$

where $\mathcal{H}(Q)$ denotes the eigenspace of the charge operator $\hat{Q}$ corresponding to the eigenvalue Q. The total charge Q of the whole system has an additive property and can be written as the sum of the charges q of its constituent subsystems. Therefore, for the bipartite system, $A\bar{A}$, a projector with a given charge Q for the whole system can be written in terms of the projectors of its constituents A and $\bar{A}$ subsystems as follows:

$$\hat{\Pi}^{(Q)}_{A\bar{A}} = \sum_{q_A + \bar{q}_{\bar{A}} = Q} \hat{\Pi}^{(q_A)}_A \otimes \hat{\Pi}^{(\bar{q})}_{\bar{A}} \ . \tag{2.2}$$

As a result, the Hilbert space $\mathcal{H}(Q)$ can be decomposed as

$$\mathcal{H}(Q) = \bigoplus_{q=0}^{Q} \mathcal{H}_A(q) \otimes \mathcal{H}_{\bar{A}}(\bar{q}), \tag{2.3}$$

where $\mathcal{H}_A(q)$ represents the eigenspace of the charge operator $\hat{Q}_A$ with an eigenvalue q, and $\mathcal{H}_{\bar{A}}(\bar{q})$ denotes the eigenspace of the charge operator $\hat{Q}_{\bar{A}}$ with an eigenvalue $\bar{q} = Q - q$. In the upcoming discussion, we will utilize the random matrix formalism and large-N diagrammatic techniques [32–34] adapted for symmetric random states to derive symmetry-resolved Page curves and symmetry-resolved relative entropy for this class of random states.

Let's begin with a symmetric Haar random pure state $|\Psi^{(Q)}\rangle$ with a definite charge Q on a bipartite Hilbert space $\mathcal{H}(Q)$, i.e., $\hat{\Pi}^{(Q')} |\Psi^{(Q)}\rangle = \delta_{Q',Q} |\Psi^{(Q)}\rangle$,

$$|\Psi^{(Q)}\rangle = \sum_{\substack{i,\alpha \\ q+\bar{q}=Q}}^{d_A(q), d_{\bar{A}}(\bar{q})} X^{(q,\bar{q})}_{i_q,\alpha_{\bar{q}}} |i_q\rangle_A \otimes |\alpha_{\bar{q}}\rangle_{\bar{A}}\,, \tag{2.4}$$

where $\{|i_q\rangle_A\}$ and $\{|\alpha_{\bar{q}}\rangle_{\bar{A}}\}$ are orthonormal bases for the sub-Hilbert spaces $\mathcal{H}_A(q)$ and $\mathcal{H}_{\bar{A}}(\bar{q})$ with dimensions $d_A(q)$ and $d_{\bar{A}}(\bar{q})$, respectively. We will assume that these sub-Hilbert spaces are independently large. The dimension of $\mathcal{H}(Q)$ is $d(Q) \equiv \dim\mathcal{H}(Q) = \sum_q d_A(q) d_{\bar{A}}(\bar{q})$.

The coefficients $X^{(q,\bar{q})}_{i_q,\alpha_{\bar{q}}}$'s are independent complex Gaussian random variables within the symmetry sector. Their joint probability distribution is defined as[1]

$$P(\{X^{(q,\bar{q})}_{i_q,\alpha_{\bar{q}}}\}) = \mathcal{Z}(Q)^{-1} \exp\left[-d_A(q) d_{\bar{A}}(\bar{q}) \mathrm{Tr}\left(X^{(q,\bar{q})} X^{(q,\bar{q})\dagger}\right)\right], \tag{2.5}$$

where $\mathcal{Z}(Q)$ is the normalization factor. $X^{(q,\bar{q})}$ represents the rectangular matrix whose elements are $X^{(q,\bar{q})}_{i_q,\alpha_{\bar{q}}}$ in the basis $\{|i_q\rangle_A\}$ and $\{|\alpha_{\bar{q}}\rangle_{\bar{A}}\}$.

It is worth noting that the joint probability $P(X)$ (eq. 2.5) is not the only joint probability that is compatible with the Haar measure. In fact, there exist multiple joint distributions that align with the uniform Haar distribution. An arbitrary random state can be represented in a fixed basis as shown in eq. (2.4). In this representation, the set of coefficients $X_{i\alpha}$ can be viewed as rows (or columns) of a unitary random matrix X that is distributed according to the Haar measure. The choice of distribution for these coefficients depends on the specific ensemble under consideration. If the joint probability distribution $P(X)$ remains invariant under the transformation $X \to UXU^{-1}$, where U is a unitary matrix, then $P(X)$ can be expressed as a function of the traces of powers of X. A common choice is:

$$P(X) \propto \exp(-\mathrm{tr}\, V(X)), \tag{2.6}$$

where $V(X)$ is an even-degree polynomial with a positive leading coefficient to ensure proper normalization and convergence [1].

The additivity of the symmetry charge implies that any reduced density matrix $\hat{\rho}_A$ obtained from a symmetric pure state $|\Psi^{(Q)}\rangle$ through partial tracing, $\hat{\rho}_A = \mathrm{Tr}_{\bar{A}} |\Psi^{(Q)}\rangle \langle\Psi^{(Q)}|$,

[1]In general, we define the ensemble of random states $|\Psi^{(Q)}\rangle$ drawn out of the uniform Haar distribution over the set of all states in $\mathcal{H}(Q)$. Within this subspace, we randomly select random pure states using a distribution of complex Gaussian random variables.

is also symmetric and can be expressed as shown in equation (1.5). The random reduced density matrix on $\mathcal{H}_A(q)$ is therefore given by

$$\rho_A(q) = \frac{X^{(q,\bar{q})}X^{(q,\bar{q})\dagger}}{\mathrm{Tr}(X^{(q,\bar{q})}X^{(q,\bar{q})\dagger})}. \tag{2.7}$$

The reduced density matrix $\rho_A(q)$ is a square matrix of size $d_A(q) \times d_A(q)$. The denominator is included to ensure the normalization condition $\mathrm{Tr}(\rho_A(q)) = 1$.

In the limit of a large Hilbert space dimension, where $d_A(q)$ and $d_{\bar{A}}(\bar{q})$ tend to infinity while maintaining a fixed ratio $\kappa \equiv \frac{d_A(q)}{d_{\bar{A}}(\bar{q})}$, the denominator becomes sharply peaked around unity, satisfying

$$\mathrm{Tr}(X^{(q,\bar{q})}X^{(q,\bar{q})\dagger}) = 1 + \delta. \tag{2.8}$$

This approximation arises from a crucial point: the normalization factor $\mathrm{Tr}(X^{(q,\bar{q})}X^{(q,\bar{q})\dagger})$ in eq. (2.7) is a random variable whose fluctuations around its mean value 1 is negligible to the leading order in $1/(d_A(q)d_{\bar{A}}(\bar{q}))$ [34, 62]. Therefore, to the leading order, the denominator can be replaced by its mean value,

$$\mathrm{Tr}(X^{(q,\bar{q})}X^{(q,\bar{q})\dagger}) \to 1, \tag{2.9}$$

leading to the approximation

$$\rho_A(q) \simeq X^{(q,\bar{q})}X^{(q,\bar{q})\dagger}. \tag{2.10}$$

This results in the Wishart ensemble's definition on each symmetry sector, establishing a direct connection between the symmetry-resolved reduced density matrix and the Wishart ensemble.

The asymptotic behavior of the reduced density matrix (2.10) is essential for simplifying calculations in large-dimensional Hilbert spaces, where fluctuations become negligible. In this limit, the eigenvalues of the reduced density matrix are approximated by the eigenvalues of the Wishart matrix. However, fluctuations in the denominator lead to corrections of the form $(1/d_A(q)d_{\bar{A}(\bar{q})})$. The impact of the normalization factor in eq. (2.7) is discussed in [34, 62], revealing that higher-order corrections to the entanglement negativity spectrum and two-point correlator deviate from those predicted by the Gaussian Unitary Ensemble (GUE).

In a diagrammatic language for random states the representation of the matrix element of the pure state density matrix $\rho = |\Psi^{(Q)}\rangle\langle\Psi^{(Q)}|$ associated with the symmetry sector is as follows:

$$[\rho]_{i_q\alpha_{\bar{q}},j_q\beta_{\bar{q}}} = \sum_{\substack{i,j,\alpha,\beta \\ q+\bar{q}=Q,q'+\bar{q}'=Q}}^{d_A(q),d_{\bar{A}}(\bar{q})} X^{(q,\bar{q})}_{i_q,\alpha_{\bar{q}}} X^{(q,\bar{q})*}_{j_{q'},\beta_{\bar{q}'}}$$

$$= \sum_{\substack{i,j,\alpha,\beta \\ q+\bar{q}=Q,q'+\bar{q}'=Q}}^{d_A(q),d_{\bar{A}}(\bar{q})}$$ 

. (2.11)

The left and right pairs of lines represent the bra and ket states, respectively. The solid and dashed lines correspond to subsystems A and $\bar{A}$, respectively. To the leading order in

$(1/d_A(q)d_{\bar{A}(\bar{q})})$, the reduced density matrix in the sector given by q is obtained by taking the partial trace over $\mathcal{H}_{\bar{A}}(\bar{q})$

$$\rho_A(q) \simeq \sum_{i_q,j_q} \sum_{\alpha_{\bar{q}}} X^{(q,\bar{q})}_{i_q,\alpha_{\bar{q}}} \, X^{(q,\bar{q})*}_{j_q,\alpha_{\bar{q}}} \;\; |i_q\rangle \langle j_q| \,, \tag{2.12}$$

with $\bar{q} = Q - q$. In diagrammatic formalism, by definition, matrix manipulations are performed at the bottom edge of the diagram, while ensemble averaging is done at the top of the diagram with appropriate propagators carrying weight. For instance, the matrix elements of the density matrix $\rho_A(q)$ are

$$[\rho_A(q)]_{i_q,j_q} = \sum_{\alpha_{\bar{q}}=1}^{d_{\bar{A}}(\bar{q})} X^{(q,\bar{q})}_{i_q,\alpha_{\bar{q}}} \, X^{(q,\bar{q})*}_{j_q,\alpha_{\bar{q}}} := \tag{2.13}$$

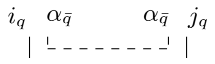

and the propagators are represented as

$$:= \langle X^{(q,\bar{q})}_{i_q,\alpha_{\bar{q}}} X^{(q',\bar{q}')*}_{j_{q'},\beta_{\bar{q}'}} \rangle = \frac{\delta_{qq'}\delta_{\bar{q}\bar{q}'}\delta_{i_q j_{q'}}\delta_{\alpha_{\bar{q}}\beta_{\bar{q}'}}}{d_A(q)d_{\bar{A}}(\bar{q})}. \tag{2.14}$$

These renormalization factors ensure that $\rho_A(q)$ has a unit trace on average. Then, take the trace of the density matrix $\rho_A(q)$ as follows:

$$\langle \mathrm{Tr}\rho_A(q) \rangle =$$

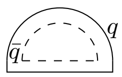

$$= d_A(q)\, d_{\bar{A}}(\bar{q}) \, \frac{1}{d_A(q)\, d_{\bar{A}}(\bar{q})} = 1, \tag{2.15}$$

The quantum numbers for each symmetry sector are explicitly displayed on the lines. Each closed loop, whether solid or dashed, contributes a factor equal to the dimension of the corresponding sector. It's important to note that, according to the diagrammatic rules for averaging, we must sum over all possible contractions of the bras and kets. Furthermore, for every insertion of the density matrix, we incorporate a factor of $(d_A(q)d_{\bar{A}}(\bar{q}))^{-1}$.

2.1 Symmetry-resolved Page's curve

To compute the ensemble average of the symmetry-resolved relative entropy, we first need to compute the ensemble average of the symmetry-resolved Rényi entropy. This can be done by representing the symmetry-resolved Rényi entropy diagrammatically as shown below:

$$\mathrm{tr}\,[\rho_A^n] = \tag{2.16}$$

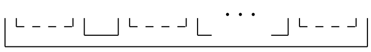

Ensemble averaging involves summing all possible contractions of the same type of bra and kets with each other. We assume that the dimensions of the sub-Hilbert spaces are large, with $d_A(q), d_{\bar{A}}(\bar{q}) \propto N \to \infty$, but their relative sizes, $d_A(q)/d_{\bar{A}}(\bar{q})$, are finite. In this limit, the dominant leading diagrams that maximize the number of loops are planar diagrams. In the double-line notation, these diagrams correspond to the standard large-N topological expansion. In the context of enumerative combinatorics and probability theory, planar diagrams correspond to non-crossing permutations. As an example, for $n = 2$, we have

$$\mathrm{Tr}(\rho_A(q))^2 = \tag{2.17}$$

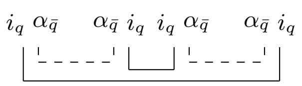

The ensemble average is calculated by summing the two possible contractions:

$$\overline{\mathrm{Tr}\rho_A(q)^2} =$$
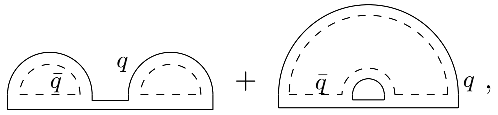

$$= \frac{1}{d_A(q)} + \frac{1}{d_{\bar{A}}(\bar{q})}. \tag{2.18}$$

Similarly, for $n = 3$, we found that

$$\overline{\mathrm{Tr}\,(\rho_A(q))^3} =$$
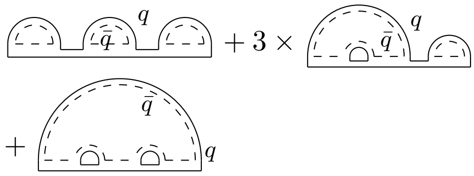

$$= \frac{1}{d_A^2(q)} + \frac{3}{d_A(q)d_{\bar{A}}(\bar{q})} + \frac{1}{d_{\bar{A}}^2(\bar{q})}. \tag{2.19}$$

Similarly, the higher moments can be computed by contracting various bras and kets of the same type with each other. In general, the sum runs over all possible contractions, so the moments can be expressed as a sum over the permutation group

$$\overline{\mathrm{Tr}\,[\rho_A^n]} = \frac{1}{(d_A(q)d_{\bar{A}}(\bar{q}))^n} \sum_{\tau \in S_n} (d_A(q))^{C(\eta^{-1}\circ\tau)} (d_{\bar{A}}(\bar{q}))^{C(\tau)}, \tag{2.20}$$

where $C(\cdot)$ represents the number of cycles in the given permutation and η denotes the cyclic permutation. Each permutation corresponds to a diagram, with the cycle structure determining which bra is contracted with which ket.

For example for $n = 2$, in eq. (2.18), the first diagram depicts the identity permutation, where each bra is contracted with its corresponding ket. In contrast, the second diagram illustrates the swap permutation, where the bra from the first density matrix is contracted with the ket from the second density matrix, and vice versa. In this case, the number of loops is $C(\eta^{-1} \circ \tau) = 2$ and $C(\tau) = 2$. These two permutations represent all the elements of the symmetric group $\mathcal{S}_2$.

Similarly, we can consider the case for $n = 3$. In eq. (2.19) the allowed permutations are denoted Within each diagram, we count the number of loops with each loop contributing a factor of the Hilbert space dimension. Once again, the first diagram represents the identity permutation where each bra is contracted with its corresponding ket. In the second diagram, the bra of the first density matrix is contracted with the ket of the second and vice versa, while the third bra is contracted with its corresponding ket. The coefficient, 3, denotes the number of permutations which yield the same diagram. In the third diagram, the contraction is as follows: the bra of the first density matrix is contracted with the ket from the second density matrix, the bra of the second density matrix is contracted with the ket from the third density matrix, and finally, the bra of the third density matrix is contracted with the ket of the first density matrix. In this case, the number of loops is $C(\eta^{-1} \circ \tau) = 3$ and $C(\tau) = 1$. These permutations belong to the symmetric group $\mathcal{S}_3$.

When the sub-Hilbert spaces are large, the contributions from non-crossing permutations become dominant. In other words, these transformations maximize the expression $C(\eta^{-1} \circ$

JHEP04(2025)090

$\tau) + C(\tau)$. For non-crossing permutations, we have $C(\eta^{-1} \circ \tau) + C(\tau) = n + 1$. The number of such permutations with $C(\eta^{-1} \circ \tau) = k$ is given by the Narayana number [63, 64].

$$N_{n,k} = \frac{1}{n}\binom{n}{k}\binom{n}{k-1}. \tag{2.21}$$

Thus, the sum in equation (2.20) can be re-expressed as:

$$\begin{aligned} \overline{\mathrm{Tr}(\rho_A(q))^n} &= \frac{1}{(d_A(q) d_{\bar{A}}(\bar{q}))^n} \sum_{k=1}^{n} N_{n,k} (d_A(q))^k (d_{\bar{A}}(\bar{q}))^{n+1-k} \\ &= (d_A(q))^{1-n}\, {}_2F_1\left(1-n, -n; 2; \frac{d_A(q)}{d_{\bar{A}}(\bar{q})}\right), \end{aligned} \tag{2.22}$$

where ${}_2F_1$ is a hypergeometric function. This expression gives the *the symmetry-resolved Page's curve* [65–67].

$$\overline{S_A(q)} = \log d_A(q) - \frac{d_A(q)}{2 d_{\bar{A}}(\bar{q})}, \tag{2.23}$$

This expression characterizes the ensemble average of bipartite symmetry-resolved entanglement entropies for ensembles of Haar-random pure states with a U(1)-symmetry. This result can be interpreted in the context of the information paradox in charged black holes [68] or thermalization in each symmetry sector.

3 Symmetry-resolved relative entropy of random states

By using a replica trick (1.12), we can compute the symmetry-resolved relative entropy. In the case of relative entropy, we have two distinct symmetry-resolved density matrices, $\rho_A(q)$ and $\sigma_A(q)$, associated with the symmetry sector q. These matrices must be averaged separately within the ensemble. To avoid confusion, we use black and red colors to represent $\rho_A(q)$ and $\sigma_A(q)$, respectively.

To calculate the symmetry-resolved relative entropy, we need to determine the diagram that represents the overlap between symmetry-resolved density matrices raised to arbitrary powers. For example, when considering two density matrices we will have diagrams like:

$$\mathrm{Tr}(\rho_A(q)\sigma_A(q)) =$$ 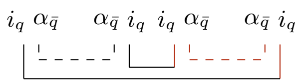 . (3.1)

There is only one term for the ensemble averaging process, as the black and red lines are averaged separately.

$$\overline{\mathrm{Tr}(\rho_A(q)\sigma_A(q))} =$$ 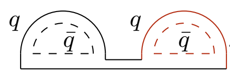, (3.2)

The above expression yields $d_A^{-1}(q)$. For higher powers of σ_A, we have the following diagram:

$$\mathrm{Tr}(\rho_A(q)\,(\sigma_A(q))^{n-1}) =$$ 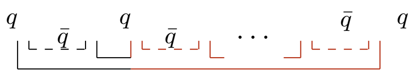 . (3.3)

JHEP04(2025)090

Due to the presence of only one copy of ρ_A, and the disallowance of contracting the black and red indices during ensemble averaging, we need to contract the first density matrix with itself. As a result, the summation runs only over a subgroup of permutations that stabilize the first element (black lines) and permute the red lines, denoted as $\mathbb{1} \times S_{n-1}$. This can be inferred from the following diagram:

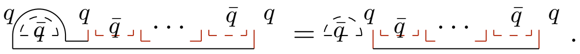

(3.4)

The ensemble average for higher powers of σ_A can be expressed as a sum over the broken permutation group, $\tau \in \mathbb{1} \times S_{n-1}$.

$$\overline{\mathrm{Tr}(\rho_A(q)(\sigma_A(q))^{n-1})} = \frac{1}{(d_A(q)d_{\bar{A}}(\bar{q}))^n} \times \sum_{\tau \in \mathbb{1} \times S_{n-1}} (d_A(q))^{C(\eta^{-1}\circ\tau)}(d_{\bar{A}}(\bar{q}))^{C(\tau)}. \tag{3.5}$$

To maximize the exponent, we should maximize the number of loops in the diagrams. The diagrams that maximize the total number of loops are noncrossing ones that only act on the $(n-1)$ red indices. The number of such non-crossing permutations NC_{n-1} with $C(\eta^{-1}\circ\tau) = k$ is given by the Narayana number $N_{n-1,k}$. Therefore, we can rewrite the sum as:

$$\overline{\mathrm{Tr}(\rho_A(q)(\sigma_A(q))^{n-1})} = \frac{1}{(d_A(q)d_{\bar{A}}(\bar{q}))^n} \times \sum_{k=1}^{n-1} N_{n-1,k}(d_A(q))^k(d_{\bar{A}}(\bar{q}))^{n+1-k},$$

The above expression can be written as a hypergeometric function

$$\overline{\mathrm{Tr}(\rho_A(q)\,(\sigma_A(q))^{n-1})} = \begin{cases} (d_A(q))^{1-n}\,{}_2F_1\left(1-n, 2-n; 2; \frac{d_A(q)}{d_{\bar{A}}(\bar{q})}\right)., & d_A(q) < (d_{\bar{A}}(\bar{q}) \\ (d_{\bar{A}}(\bar{q}))^{2-n}(d_A(q))^{-1}\,{}_2F_1\left(1-n, 2-n; 2; \frac{d_{\bar{A}}(\bar{q})}{d_A(q)}\right), & d_A(q) > d_{\bar{A}}(\bar{q}) \end{cases} \tag{3.6}$$

Taking the $n \to 1$ limit, we find

$$\lim_{n\to 1} \frac{1}{1-n} \overline{\log\left(\mathrm{Tr}(\rho_A(q)\,(\sigma_A(q))^{n-1})\right)} \tag{3.7}$$

$$= \begin{cases} \log\left(d_A(q)\right) + 1 + \left(\frac{d_{\bar{A}}(\bar{q})}{d_A(q)} - 1\right)\log\left(1 - \frac{d_A(q)}{d_{\bar{A}}(\bar{q})}\right), & d_A(q) < d_{\bar{A}}(\bar{q}) \\ \infty, & d_{\bar{A}}(\bar{q}) < d_A(q) \end{cases}. \tag{3.8}$$

Therefore, the ensemble average of the symmetry-resolved relative entropy is obtained by[2]

$$\overline{D(\rho_A||\sigma_A)} = \begin{cases} 1 + \frac{d_A(q)}{2d_{\bar{A}}(\bar{q})} + \left(\frac{d_{\bar{A}}(\bar{q})}{d_A(q)} - 1\right)\log\left(1 - \frac{d_A(q)}{d_{\bar{A}}(\bar{q})}\right), & d_A(q) < d_{\bar{A}}(\bar{q}) \\ \infty, & d_A(q) > d_{\bar{A}}(\bar{q}) \end{cases}. \tag{3.9}$$

This formula represents the final result of symmetry-resolved relative entropy for Haar random states. It shows that quite generally equipartition is broken, i.e. it depends on the symmetry sector q.

When the ratio $d_A(q)/d_{\bar{A}}(\bar{q})$ is very small, $d_A(q)/d_{\bar{A}}(\bar{q}) \ll 1$, the symmetry-resolved relative entropy can be approximated as $\overline{D(\rho_A||\sigma_A)} \approx d_A(q)/d_{\bar{A}}(\bar{q})$. This approximation

[2]In general, the ensemble average and logarithm do not commute, so a further replica trick is needed. However, in the case of large Hilbert space dimensions, these operations approximately commute [32].

suggests that the symmetry-resolved density matrices become almost indistinguishable when we have limited information about the symmetry sector, as we would expect. The symmetry-resolved relative entropy increases monotonically as $d_A(q)/d_{\bar{A}}(\bar{q})$ increases, and it approaches a value of $3/2$ as $d_A(q)$ approaches $d_{\bar{A}}(\bar{q})$. This behavior reflects the monotonicity of symmetry-resolved relative entropy under the partial trace.

For $d_A(q) > d_{\bar{A}}(\bar{q})$, the symmetry-resolved relative entropy becomes infinite. This can be understood as follows: in general, the quantum relative entropy $D(\rho \parallel \sigma)$ becomes infinite when the support of ρ lies entirely outside the support of σ; that is, $\mathrm{supp}(\rho_A) \nsubseteq \mathrm{supp}(\sigma_A)$. In such cases, the two states ρ and σ are perfectly distinguishable, meaning there exists a measurement strategy that can identify the state with zero error probability.

In the context of the symmetry-resolved relative entropy of random states, the Wishart ensemble has a rank of at most $\min(d_A(q), d_{\bar{A}}(\bar{q}))$. When $d_A(q) > d_{\bar{A}}(\bar{q})$, every reduced state on $\mathcal{H}_A(q)$ in the ensemble will have a deficiency in rank, resulting in $d_A(q) - d_{\bar{A}}(\bar{q})$ zero eigenvalues. Consequently, the support of $\rho_A(q)$ will not be contained within the support of $\sigma_A(q)$. This is why the symmetry-resolved relative entropy becomes formally infinite in this regime.

In the following, we will briefly discuss the implications of eq. (3.9) for quantum hypothesis testing, which is one of the most fundamental processes in information processing. This process represents the operational meaning of quantum relative entropy [69, 70]. Given a quantum state that is either ρ or σ, the goal is to determine which state is present using quantum measurements. Quantum Stein's Lemma states that the optimal asymptotic error rate in distinguishing these states is given by $e^{-D(\rho\|\sigma)}$ [69, 70]. When access to a quantum system is limited to a sub-Hilbert space A, the error rate in hypothesis testing exhibits distinct behaviors:

- **Majority access**: if A spans more than half of the total Hilbert space, the error probability asymptotically vanishes.
- **Minority access**: if A spans less than half the total space, the error probability converges to a finite value, exponentially close to the maximal error rate.

This behavior arises from the interplay between system size and entropy. Larger accessible subspaces provide more information about the quantum state, reducing uncertainty and improving distinguishability.

This scenario can be adjusted to the case where there is global symmetry by implicating it to symmetry sectors and giving operational meaning to symmetry-resolved relative entropy. Let's consider a state on $\mathcal{H}_A(q)$, which could be either $\rho(q)$ or $\sigma(q)$, and we want to determine which state we have been given. The refined quantum Stein's lemma[3] for each symmetry sector tells us that determining which state we have is given by $e^{-D(\rho(q)\|\sigma(q))}$. Therefore, eq. (3.9) indicates that if we only have partial information about the state in each sector (access to sub-sector $\mathcal{H}_A(q)$), for a measure one set of quantum states on each symmetry sector, the error will either vanish if the sub-sector $\mathcal{H}_A(q)$ is larger than half the total sector $\mathcal{H}_A(q) \otimes \mathcal{H}_{\bar{A}}(\bar{q})$, or

[3]Here, we refer to the application of the quantum Stein's lemma in the symmetry sector as a refined version of the quantum Stein's lemma.

JHEP04(2025)090

it will be finite and exponentially close (in the entropy) to the maximal error rate if $\mathcal{H}_A(q)$ is smaller than half the total sector size. The lemma defines the optimal asymptotic error rate.

4 Conclusion

In this manuscript, we have utilized a large-N diagrammatic technique to calculate symmetry-resolved relative entropies, which serve as a measure of distinguishability within a given symmetry sector. Our focus has been on U(1) symmetric random states drawn from the Wishart ensemble. By using the replica trick formalism, we have obtained the symmetry-resolved Page's curve and symmetry-resolved relative entropies. These results deepen our understanding of the properties of these random states.

In general, we have found that relative entropies violate entanglement equipartition in the symmetry resolution for Haar-random states. Our results have shown that within each symmetry sector, in the Abelian case, the symmetry-resolved relative entropy monotonically increases with $d_A(q)/d_{\bar{A}}(\bar{q})$ and reaches a value of 3/2 when $d_A(q) = d_{\bar{A}}(\bar{q})$. This behavior demonstrates the monotonicity of symmetry-resolved relative entropy under the partial trace. Moreover, we found that when $d_A(q) > d_{\bar{A}}(\bar{q})$, the symmetry-resolved relative entropy becomes formally infinite. This can be understood as follows.

For $d_A(q) < d_{\bar{A}}(\bar{q})$, the symmetry-resolved reduced density matrices have full rank, matching the rank of the Wishart ensemble, resulting in a finite symmetry-resolved relative entropy. On the other hand, the symmetry-resolved relative entropy becomes infinite when $d_A(q) > d_{\bar{A}}(\bar{q})$ due to a rank deficiency in the entanglement spectrum. In this case, within the Wishart ensemble, there are a finite number of states that are inaccessible to either $\rho_A(q)$ or $\sigma_A(q)$ due to a rank deficiency (zero eigenvalues) leading to different supports. Consequently, this results in an infinite symmetry-resolved relative entropy. For instance, if $d_A(q) = d_{\bar{A}}(\bar{q}) + 1$, it indicates that there is a single zero eigenvalue in the spectrum of the reduced density matrix. This suggests that a state is inaccessible to either $\rho_A(q)$ or $\sigma_A(q)$, leading to different supports for the density matrices and resulting in an infinite symmetry-resolved relative entropy.

For instance, in the context of an evaporating black hole, the authors [71] utilized asymmetry tools [72] to examine how asymmetry evolves in the emitted radiation. They found that the emitted radiation remains symmetric until the Page time, even in the absence of any inherent symmetry. However, shortly after this threshold, the radiation undergoes symmetry breaking. This phenomenon can be understood within the framework of the symmetry sector. Before the Page time, the radiation exhibits symmetry, which leads to a finite symmetry-resolved relative entropy. After the Page time, global symmetry is broken, and symmetric states are no longer present. This shift is evidenced by the infinite violation of the symmetry-resolved relative entropy due to a rank deficiency in the entanglement spectrum.

The infinity of relative entropy for random states has also been observed in the work [32] as well as in the context of holography and JT gravity [73]. In JT gravity, there is a finite number of states accessible, resulting in a rank deficiency (zero eigenvalues) after the Page time and an infinite relative entropy as discussed in the work [73]. Moreover, the abrupt shift in the radiation from a symmetric to a nonsymmetric state has been observed in ref. [74]

JHEP04(2025)090

within the framework of a particular gravity theory, utilizing the replica wormhole formalism. It is valuable to investigate these works through the lens of symmetry-resolved relative entropy.

It would be interesting to generalize our formalism to non-abelian random states [75], the asymmetric case [72] for random states [71] or compute the *Symmetry-resolved sandwiched Rényi relative entropies* [76] for random states. We will go back to these problems in the near future.

Acknowledgments

It is my pleasure to thank Pasquale Calabrese, Sepideh Mohammadi, Ahmad Moradpouri, and Sara Murciano for reading our manuscript and providing insightful comments. I am also grateful to JHEP referee who made several very helpful suggestions that improved our manuscript.

Data Availability Statement. This article has no associated data or the data will not be deposited.

Code Availability Statement. This article has no associated code or the code will not be deposited.

References

[1] M.L. Mehta, *Random Matrices*, *Pure Appl. Math.* **142** (2004).

[2] P.J. Forrester, *Log-Gases and Random Matrices*, Princeton University Press (2010).

[3] B. Eynard, T. Kimura and S. Ribault, *Random matrices*, arXiv:1510.04430 [INSPIRE].

[4] L. D'Alessio, Y. Kafri, A. Polkovnikov and M. Rigol, *From quantum chaos and eigenstate thermalization to statistical mechanics and thermodynamics*, *Adv. Phys.* **65** (2016) 239 [arXiv:1509.06411] [INSPIRE].

[5] B. Collins and I. Nechita, *Random matrix techniques in quantum information theory*, *J. Math. Phys.* **57** (2016) 015215 [INSPIRE].

[6] S. Popescu, A.J. Short and A. Winter, *Entanglement and the foundations of statistical mechanics*, *Nature Phys.* **2** (2006) 754 [INSPIRE].

[7] C. Gogolin and J. Eisert, *Equilibration, thermalisation, and the emergence of statistical mechanics in closed quantum systems*, *Rept. Prog. Phys.* **79** (2016) 056001 [arXiv:1503.07538] [INSPIRE].

[8] D.N. Page, *Information in black hole radiation*, *Phys. Rev. Lett.* **71** (1993) 3743 [hep-th/9306083] [INSPIRE].

[9] P. Hayden and J. Preskill, *Black holes as mirrors: quantum information in random subsystems*, *JHEP* **09** (2007) 120 [arXiv:0708.4025] [INSPIRE].

[10] D.N. Page, *Average entropy of a subsystem*, *Phys. Rev. Lett.* **71** (1993) 1291 [gr-qc/9305007] [INSPIRE].

[11] E. Bianchi et al., *Volume-Law Entanglement Entropy of Typical Pure Quantum States*, *PRX Quantum* **3** (2022) 030201 [arXiv:2112.06959] [INSPIRE].

[12] V. Vedral, *The role of relative entropy in quantum information theory*, *Rev. Mod. Phys.* **74** (2002) 197 [quant-ph/0102094] [INSPIRE].

[13] A. Wehrl, *General properties of entropy*, *Rev. Mod. Phys.* **50** (1978) 221 [INSPIRE].

[14] T. Faulkner, R.G. Leigh, O. Parrikar and H. Wang, *Modular Hamiltonians for Deformed Half-Spaces and the Averaged Null Energy Condition*, *JHEP* **09** (2016) 038 [arXiv:1605.08072] [INSPIRE].

[15] S. Balakrishnan, T. Faulkner, Z.U. Khandker and H. Wang, *A General Proof of the Quantum Null Energy Condition*, *JHEP* **09** (2019) 020 [arXiv:1706.09432] [INSPIRE].

[16] H. Casini, E. Teste and G. Torroba, *Relative entropy and the RG flow*, *JHEP* **03** (2017) 089 [arXiv:1611.00016] [INSPIRE].

[17] H. Casini, S. Grillo and D. Pontello, *Relative entropy for coherent states from Araki formula*, *Phys. Rev. D* **99** (2019) 125020 [arXiv:1903.00109] [INSPIRE].

[18] N. Lashkari, *Relative Entropies in Conformal Field Theory*, *Phys. Rev. Lett.* **113** (2014) 051602 [arXiv:1404.3216] [INSPIRE].

[19] N. Lashkari, *Modular Hamiltonian for Excited States in Conformal Field Theory*, *Phys. Rev. Lett.* **117** (2016) 041601 [arXiv:1508.03506] [INSPIRE].

[20] P. Ruggiero and P. Calabrese, *Relative Entanglement Entropies in 1+1-dimensional conformal field theories*, *JHEP* **02** (2017) 039 [arXiv:1612.00659] [INSPIRE].

[21] G. Sárosi and T. Ugajin, *Relative entropy of excited states in two dimensional conformal field theories*, *JHEP* **07** (2016) 114 [arXiv:1603.03057] [INSPIRE].

[22] M. Ghasemi, *Left-Right Relative Entropy*, arXiv:2411.09406 [INSPIRE].

[23] D.D. Blanco, H. Casini, L.-Y. Hung and R.C. Myers, *Relative Entropy and Holography*, *JHEP* **08** (2013) 060 [arXiv:1305.3182] [INSPIRE].

[24] D.L. Jafferis and S.J. Suh, *The Gravity Duals of Modular Hamiltonians*, *JHEP* **09** (2016) 068 [arXiv:1412.8465] [INSPIRE].

[25] D.L. Jafferis, A. Lewkowycz, J. Maldacena and S.J. Suh, *Relative entropy equals bulk relative entropy*, *JHEP* **06** (2016) 004 [arXiv:1512.06431] [INSPIRE].

[26] N. Lashkari et al., *Gravitational positive energy theorems from information inequalities*, *PTEP* **2016** (2016) 12C109 [arXiv:1605.01075] [INSPIRE].

[27] H. Casini, *Relative entropy and the Bekenstein bound*, *Class. Quant. Grav.* **25** (2008) 205021 [arXiv:0804.2182] [INSPIRE].

[28] A.C. Wall, *A proof of the generalized second law for rapidly changing fields and arbitrary horizon slices*, *Phys. Rev. D* **85** (2012) 104049 [*Erratum ibid.* **87** (2013) 069904] [arXiv:1105.3445] [INSPIRE].

[29] R. Bousso, H. Casini, Z. Fisher and J. Maldacena, *Proof of a Quantum Bousso Bound*, *Phys. Rev. D* **90** (2014) 044002 [arXiv:1404.5635] [INSPIRE].

JHEP04(2025)090

[30] R. Bousso, H. Casini, Z. Fisher and J. Maldacena, *Entropy on a null surface for interacting quantum field theories and the Bousso bound*, Phys. Rev. D **91** (2015) 084030 [arXiv:1406.4545] [INSPIRE].

[31] R. Longo and F. Xu, *Comment on the Bekenstein bound*, J. Geom. Phys. **130** (2018) 113 [arXiv:1802.07184] [INSPIRE].

[32] J. Kudler-Flam, *Relative Entropy of Random States and Black Holes*, Phys. Rev. Lett. **126** (2021) 171603 [arXiv:2102.05053] [INSPIRE].

[33] J. Kudler-Flam, V. Narovlansky and S. Ryu, *Distinguishing Random and Black Hole Microstates*, PRX Quantum **2** (2021) 040340 [arXiv:2108.00011] [INSPIRE].

[34] H. Shapourian, S. Liu, J. Kudler-Flam and A. Vishwanath, *Entanglement Negativity Spectrum of Random Mixed States: a Diagrammatic Approach*, PRXQuantum **2** (2021) 030347 [arXiv:2011.01277] [INSPIRE].

[35] G. Lindblad, *Completely positive maps and entropy inequalities*, Commun. Math. Phys. **40** (1975) 147 [INSPIRE].

[36] M. Goldstein and E. Sela, *Symmetry-resolved entanglement in many-body systems*, Phys. Rev. Lett. **120** (2018) 200602 [arXiv:1711.09418] [INSPIRE].

[37] A. Lukin et al., *Probing entanglement in a many-body–localized system*, Science **364** (2019) aau0818 [INSPIRE].

[38] H.M. Wiseman and J.A. Vaccaro, *Entanglement of Indistinguishable Particles Shared between Two Parties*, Phys. Rev. Lett. **91** (2003) 097902 [INSPIRE].

[39] H. Barghathi, C.M. Herdman and A.D. Maestro, *Rényi Generalization of the Accessible Entanglement Entropy*, Phys. Rev. Lett. **121** (2018) 150501 [INSPIRE].

[40] M. Kiefer-Emmanouilidis, R. Unanyan, M. Fleischhauer and J. Sirker, *Evidence for Unbounded Growth of the Number Entropy in Many-Body Localized Phases*, Phys. Rev. Lett. **124** (2020) 243601 [arXiv:2003.04849] [INSPIRE].

[41] J.C. Xavier, F.C. Alcaraz and G. Sierra, *Equipartition of the entanglement entropy*, Phys. Rev. B **98** (2018) 041106 [arXiv:1804.06357] [INSPIRE].

[42] L. Capizzi, P. Ruggiero and P. Calabrese, *Symmetry resolved entanglement entropy of excited states in a CFT*, J. Stat. Mech. **2007** (2020) 073101 [arXiv:2003.04670] [INSPIRE].

[43] P. Calabrese, J. Dubail and S. Murciano, *Symmetry-resolved entanglement entropy in Wess-Zumino-Witten models*, JHEP **10** (2021) 067 [arXiv:2106.15946] [INSPIRE].

[44] M. Ghasemi, *Universal thermal corrections to symmetry-resolved entanglement entropy and full counting statistics*, JHEP **05** (2023) 209 [arXiv:2203.06708] [INSPIRE].

[45] F. Ares, P. Calabrese, G. Di Giulio and S. Murciano, *Multi-charged moments of two intervals in conformal field theory*, JHEP **09** (2022) 051 [arXiv:2206.01534] [INSPIRE].

[46] G. Di Giulio et al., *On the boundary conformal field theory approach to symmetry-resolved entanglement*, SciPost Phys. Core **6** (2023) 049 [arXiv:2212.09767] [INSPIRE].

[47] Y. Kusuki, S. Murciano, H. Ooguri and S. Pal, *Symmetry-resolved entanglement entropy, spectra & boundary conformal field theory*, JHEP **11** (2023) 216 [arXiv:2309.03287] [INSPIRE].

[48] H. Gaur and U.A. Yajnik, *Multi-charged moments and symmetry-resolved Rényi entropy of free compact boson for multiple disjoint intervals*, JHEP **01** (2024) 042 [arXiv:2310.14186] [INSPIRE].

JHEP04(2025)090

[49] N. Laflorencie and S. Rachel, *Spin-resolved entanglement spectroscopy of critical spin chains and Luttinger liquids*, J. Phys. A **2014** (2014) P11013 [INSPIRE].

[50] A. Belin et al., *Holographic Charged Renyi Entropies*, JHEP **12** (2013) 059 [arXiv:1310.4180] [INSPIRE].

[51] S. Zhao, C. Northe and R. Meyer, *Symmetry-resolved entanglement in AdS_3/CFT_2 coupled to U(1) Chern-Simons theory*, JHEP **07** (2021) 030 [arXiv:2012.11274] [INSPIRE].

[52] K. Weisenberger, S. Zhao, C. Northe and R. Meyer, *Symmetry-resolved entanglement for excited states and two entangling intervals in AdS_3/CFT_2*, JHEP **12** (2021) 104 [arXiv:2108.09210] [INSPIRE].

[53] S. Zhao, C. Northe, K. Weisenberger and R. Meyer, *Charged moments in W_3 higher spin holography*, JHEP **05** (2022) 166 [arXiv:2202.11111] [INSPIRE].

[54] G. Di Giulio and J. Erdmenger, *Symmetry-resolved modular correlation functions in free fermionic theories*, JHEP **07** (2023) 058 [arXiv:2305.02343] [INSPIRE].

[55] A. Milekhin and A. Tajdini, *Charge fluctuation entropy of Hawking radiation: a replica-free way to find large entropy*, SciPost Phys. **14** (2023) 172 [arXiv:2109.03841] [INSPIRE].

[56] K. Hejazi and H. Shapourian, *Symmetry-protected entanglement in random mixed states*, Phys. Rev. A **106** (2022) 052428 [arXiv:2112.00032] [INSPIRE].

[57] D.X. Horvath, S. Fraenkel, S. Scopa and C. Rylands, *Charge-resolved entanglement in the presence of topological defects*, Phys. Rev. B **108** (2023) 165406 [arXiv:2306.15532] [INSPIRE].

[58] M. Fossati, F. Ares and P. Calabrese, *Symmetry-resolved entanglement in critical non-Hermitian systems*, Phys. Rev. B **107** (2023) 205153 [arXiv:2303.05232] [INSPIRE].

[59] N. Feldman, J. Knaute, E. Zohar and M. Goldstein, *Superselection-resolved entanglement in lattice gauge theories: a tensor network approach*, JHEP **05** (2024) 083 [arXiv:2401.01942] [INSPIRE].

[60] H.-H. Chen, *Symmetry decomposition of relative entropies in conformal field theory*, JHEP **07** (2021) 084 [arXiv:2104.03102] [INSPIRE].

[61] L. Capizzi and P. Calabrese, *Symmetry resolved relative entropies and distances in conformal field theory*, JHEP **10** (2021) 195 [arXiv:2105.08596] [INSPIRE].

[62] X. Chen and A.W.W. Ludwig, *Universal Spectral Correlations in the Chaotic Wave Function, and the Development of Quantum Chaos*, Phys. Rev. B **98** (2018) 064309 [arXiv:1710.02686] [INSPIRE].

[63] G. Kreweras, Sur les partitions non croisees d'un cycle, *Discrete Mathematics* **1** (1972) 333.

[64] R. Simion, *Noncrossing partitions*, *Discrete Math.* **217** (2000) 367.

[65] E. Bianchi and P. Dona, *Typical entanglement entropy in the presence of a center: page curve and its variance*, Phys. Rev. D **100** (2019) 105010 [arXiv:1904.08370] [INSPIRE].

[66] S. Murciano, P. Calabrese and L. Piroli, *Symmetry-resolved Page curves*, Phys. Rev. D **106** (2022) 046015 [arXiv:2206.05083] [INSPIRE].

[67] P.H.C. Lau, T. Noumi, Y. Takii and K. Tamaoka, *Page curve and symmetries*, JHEP **10** (2022) 015 [arXiv:2206.09633] [INSPIRE].

[68] P. Li and Y. Ling, *Refined symmetry-resolved Page curve and charged black holes*, Chin. Phys. C **48** (2024) 053109 [arXiv:2311.04436] [INSPIRE].

JHEP04(2025)090

[69] F. Hiai and D. Petz, *The proper formula for relative entropy and its asymptotics in quantum probability*, *Commun. Math. Phys.* **143** (1991) 99 [INSPIRE].

[70] T. Ogawa and H. Nagaoka, *Strong converse and stein's lemma in the quantum hypothesis testing*, in H. Masahito ed., *Asymptotic Theory of Quantum Statistical Inference: Selected Papers*, World Scientific Publishing Co. Pte. Ltd (2005), pp. 28-42, DOI:10.1142/9789812563071_0003 [quant-ph/9906090] [INSPIRE].

[71] F. Ares, S. Murciano, L. Piroli and P. Calabrese, *Entanglement asymmetry study of black hole radiation*, *Phys. Rev. D* **110** (2024) L061901 [arXiv:2311.12683] [INSPIRE].

[72] F. Ares, S. Murciano and P. Calabrese, *Entanglement asymmetry as a probe of symmetry breaking*, *Nature Commun.* **14** (2023) 2036 [arXiv:2207.14693] [INSPIRE].

[73] J. Kudler-Flam and P. Rath, *Large and small corrections to the JLMS Formula from replica wormholes*, *JHEP* **08** (2022) 189 [arXiv:2203.11954] [INSPIRE].

[74] Y. Chen and H.W. Lin, *Signatures of global symmetry violation in relative entropies and replica wormholes*, *JHEP* **03** (2021) 040 [arXiv:2011.06005] [INSPIRE].

[75] E. Bianchi, P. Dona and R. Kumar, *Non-Abelian symmetry-resolved entanglement entropy*, *SciPost Phys.* **17** (2024) 127 [arXiv:2405.00597] [INSPIRE].

[76] M. Ghasemi, *Symmetry-resolved sandwiched Rényi relative entropies of random states*, in progress.